

Bidirectional gut-to-brain and brain-to-gut propagation of synucleinopathy in non-human primates

 Marie-Laure Arotcarena,^{1,2,*}
 Sandra Dovero,^{1,2,*}
 Alice Prigent,^{3,4,5,*}
 Mathieu Bourdenx,^{1,2,*,§}
 Sandrine Camus,^{1,2} Gregory Porras,^{1,2} Marie-Laure Thiolat,^{1,2}
 Maddalena Tasselli,^{3,4,5} Philippe Aubert,^{3,4,5} Niels Kruse,^{6,7} Brit Mollenhauer,^{6,7}
 Ines Trigo Damas,^{8,9,10} Cristina Estrada,^{11,12} Nuria Garcia-Carrillo,¹³
 Nishant N. Vaikath,¹⁴ Omar M.A. El-Agnaf,¹⁴ Maria Trinidad Herrero,^{11,12} Miquel Vila,^{15,16,17}
 Jose A. Obeso,^{8,9,10} Pascal Derkinderen,^{3,4,5}
 Benjamin Dehay^{1,2,#} and
  Erwan Bezdard^{1,2, #}

*,#These authors contributed equally to this work.

In Parkinson's disease, synucleinopathy is hypothesized to spread from the enteric nervous system, via the vagus nerve, to the CNS. Here, we compare, in baboon monkeys, the pathological consequences of either intrastratial or enteric injection of α -synuclein-containing Lewy body extracts from patients with Parkinson's disease. This study shows that patient-derived α -synuclein aggregates are able to induce nigrostriatal lesions and enteric nervous system pathology after either enteric or striatal injection in a non-human primate model. This finding suggests that the progression of α -synuclein pathology might be either caudo-rostral or rostro-caudal, varying between patients and disease subtypes. In addition, we report that α -synuclein pathological lesions were not found in the vagal nerve in our experimental setting. This study does not support the hypothesis of a transmission of α -synuclein pathology through the vagus nerve and the dorsal motor nucleus of the vagus. Instead, our results suggest a possible systemic mechanism in which the general circulation would act as a route for long-distance bidirectional transmission of endogenous α -synuclein between the enteric and the central nervous systems. Taken together, our study provides invaluable primate data exploring the role of the gut-brain axis in the initiation and propagation of Parkinson's disease pathology and should open the door to the development and testing of new therapeutic approaches aimed at interfering with the development of sporadic Parkinson's disease.

- 1 University of Bordeaux, Neurodegenerative Diseases Institute, UMR 5293, F-33000 Bordeaux, France
- 2 CNRS, Neurodegenerative Diseases Institute, UMR 5293, F-33000 Bordeaux, France
- 3 Inserm, U1235, Nantes F-44035, France
- 4 Nantes University, Nantes F-44035, France
- 5 CHU Nantes, Department of Neurology, Nantes F-44093, France
- 6 Paracelsus-Elena-Klinik, Kassel, Germany
- 7 University Medical Center Goettingen, Institute of Neuropathology, Goettingen, Germany
- 8 HM CINAC, HM Puerta del Sur, San Pablo University Madrid, E-28938 Mostoles, Spain
- 9 Center for Networked Biomedical Research on Neurodegenerative Diseases (CIBERNED), Instituto Carlos III, Madrid, Spain
- 10 CEU, San Pablo University Madrid, E-28938 Mostoles, Spain
- 11 Clinical and Experimental Neuroscience Unit, School of Medicine, Biomedical Research Institute of Murcia (IMIB), University of Murcia, Campus Mare Nostrum, 30100 Murcia, Spain
- 12 Institute of Research on Aging (IUIE), School of Medicine, University of Murcia, 30100 Murcia, Spain
- 13 Centro Experimental en Investigaciones Biomédica (CEIB), University of Murcia, Murcia, Spain

Received January 21, 2020. Accepted March 17, 2020. Advance access publication May 7, 2020

© The Author(s) (2020). Published by Oxford University Press on behalf of the Guarantors of Brain. All rights reserved.

For permissions, please email: journals.permissions@oup.com

- 14 Neurological Disorders Research Center, Qatar Biomedical Research Institute (QBRI), Hamad Bin Khalifa University (HBKU), Education City, Qatar
- 15 Neurodegenerative Diseases Research Group, Vall d'Hebron Research Institute (VHIR)-Center for Networked Biomedical Research on Neurodegenerative Diseases (CIBERNED), Barcelona, Spain
- 16 Department of Biochemistry and Molecular Biology, Autonomous University of Barcelona (UAB), Barcelona, Spain
- 17 Catalan Institution for Research and Advanced Studies (ICREA), Barcelona, Spain

[§]Present address: Albert Einstein College of Medicine, Department of Developmental and Molecular Biology, NY, USA

Correspondence to: Dr Benjamin Dehay
Institute of Neurodegenerative Diseases, Université de Bordeaux, CNRS UMR 5293, Centre
Broca Nouvelle-Aquitaine, 146 rue Léo Saignat, 33076 Bordeaux cedex, France
E-mail: benjamin.dehay@u-bordeaux.fr

Correspondence may also be addressed to: Dr Erwan Bezard
E-mail: erwan.bezard@u-bordeaux.fr

Keywords: Parkinson's disease; α -synuclein; neurodegeneration; gut; monkey

Abbreviations: dmnX = dorsal motor nucleus of the vagus; ENS = enteric nervous system; NSE = neuron-specific enolase; SNpc = substantia nigra pars compacta

Introduction

Parkinson's disease is a common neurodegenerative disease characterized by classical motor features, but non-motor manifestations are common well before diagnosis can be established. Gastrointestinal symptoms occur in the majority of Parkinson's disease patients and constipation is among the most common early symptoms (Edwards *et al.*, 1992; Knudsen *et al.*, 2017). Autopsy studies have consistently shown that Lewy bodies and neurites, two main histological hallmarks of the neurodegeneration, are found in the enteric nervous system (ENS) in nearly every case examined (Beach *et al.*, 2010). Based on the topographic distribution of Lewy bodies, Braak and co-workers posited that Parkinson's disease pathology may begin in the gastrointestinal tract and then spread to the brain via the vagus nerve (Braak *et al.*, 2003, 2006). This hypothesis is supported by experimental data showing that misfolded α -synuclein, which is the main component of Lewy bodies, can transfer from gut to brain either after viral vector delivery of α -synuclein or recombinant α -synuclein preformed fibrils injected into the gastrointestinal tract (Ulusoy *et al.*, 2013, 2017; Holmqvist *et al.*, 2014; Manfredsson *et al.*, 2018; Uemura *et al.*, 2018). However, in these experimental models, no severe synucleinopathy or neurodegeneration was observed, which could be explained by either the time of examination after injection (a maximum of 1 year) and/or the pathogenic nature of the material used. Although appealing, the so-called 'Braak hypothesis' is still widely debated (Lionnet *et al.*, 2018). Therefore, we set out to examine a possible alternative scenario in which α -synucleinopathy might not only spread rostrally but also caudally, i.e. both from the gut to the brain and also from the brain to the gut. We hypothesized that, in non-human primates, the striatal or ENS injection of α -synuclein-containing Lewy body extracts from Parkinson's

disease patients might result in ENS and CNS pathologies, respectively.

Materials and methods

Purification of Lewy bodies from human Parkinson's disease brain

The samples were obtained from brains collected as part of the Brain Donation Program of the Brain Bank 'GIE NeuroCEB' run by a consortium of Patients Associations: ARSEP (association for research on multiple sclerosis), CSC (cerebellar ataxias), France Alzheimer and France Parkinson. The consent documents were signed by the patients themselves or their next of kin in their name, in accordance with the French Bioethical Laws. The Brain Bank GIE NeuroCEB (Bioresource Research Impact Factor number BB-0033-00011) has been declared at the Ministry of Higher Education and Research and has received approval to distribute samples (agreement AC-2013-1887). Human substantia nigra pars compacta (SNpc) was dissected from fresh frozen post-mortem midbrain samples from five patients with sporadic Parkinson's disease exhibiting conspicuous nigral Lewy body pathology on neuropathological examination (mean age at death: 75 ± 2.75 years; frozen post-mortem interval: 31.8 ± 7.45 h; GIE Neuro-CEB BB-0033-00011). Tissue was homogenized in nine volumes (w/v) ice-cold MSE buffer (10 mM MOPS/KOH, pH 7.4, 1 M sucrose, 1 mM EGTA, 1 mM EDTA) with protease inhibitor cocktail (Complete Mini; Boehringer Mannheim) with 12 strokes of a motor-driven glass/Teflon homogenizer. For Lewy body purification, a sucrose step gradient was prepared by overlaying 2.2 M with 1.4 M and finally with 1.2 M sucrose in volume ratios of 3.5:8:8 (v/v). The homogenate was layered on the gradient and centrifuged at 160 000g for 3 h using a SW32.1 rotor (Beckman). Twenty-six fractions of 1500 μ l were collected from each gradient from top (fraction 1) to bottom (fraction 26) and analysed for the

presence of α -synuclein aggregates by filter retardation assay, as previously described (Recasens et al., 2014). Further characterization of Lewy body fractions was performed by immunofluorescence, α -synuclein ELISA quantification and electron microscopy as previously described (Recasens et al., 2014). For stereotactic inoculations, Lewy body-containing fractions from patients with Parkinson's disease were mixed together in the same proportion (PD#1, fractions 19 and 20; PD#2, fractions 19 and 20; PD#3, fraction 22; PD#4, fractions 17,18 and 19; PD#5, fractions 20, 21 and 23). Lewy body fractions were adjusted to ~ 24 pg α -synuclein per microlitre of inoculated sample, as measured by a specific ELISA kit against human α -synuclein (Invitrogen, #KHB0061) according to the manufacturer's instructions. In all cases, samples were bath-sonicated for 5 min prior to *in vitro* and *in vivo* inoculations.

Ethics statement

Experiments were performed in accordance with the European Union directive of 22 September 2010 (2010/63/EU) on the protection of animals used for scientific purposes. The Institutional Animal Care and Ethical Committee of Murcia University (Spain) approved experiments under the license number REGA ES300305440012.

Monkeys and inoculations

Animals were sourced from the research animal facility of the University of Murcia (Murcia, Spain) and housed in two multi-male, multi-female exterior aviaries at a breeding farm. Animals were fed fruit, vegetables and monkey pellets twice a day before 9 am and after 5 pm. Water was available *ad libitum*. Fourteen healthy adult olive baboons (*Papio papio*) (nine male and seven female) at different ages were used in this study to reach statistically significant numbers while complying with 3R policy: young (1–3 years old, $n = 4$), adult (3–7 years old, $n = 5$), mature (7–14 years old, $n = 5$). Group sizes were chosen assuming a one-tailed alpha of 0.05, with sample size of at least three per group, which provided $> 80\%$ power to detect a difference between the treatment groups and the control group, using a Fisher's exact test. Animals were randomized into treatment or control groups. Four baboons were used for intrastriatal inoculations, five were used for enteric inoculations and five were untreated control animals. Intrastriatal inoculations of Lewy body fractions were performed at two rostrocaudal levels of the motor striatum (anterior commissure, -1 mm and -5 mm) under stereotactic guidance as previously described (Ahmed et al., 2010; Fasano et al., 2010; Porras et al., 2012; Urs et al., 2015). The total inoculated volume per hemisphere was 100 μ l (two inoculation sites with 50 μ l each at 3 μ l/min at each location site). After each inoculation, the syringe was left in place for 10 min to prevent leakage along the needle track. For inoculation of Lewy bodies into the stomach and duodenum ventral wall, the abdominal wall was opened and both stomach and duodenum were exposed as per published procedures (Miwa et al., 2006). Administration of Lewy bodies was performed using a 30-G needle slowly inserted into the ventral wall of the stomach and duodenum (Miwa et al., 2006). To ensure that the solution spreads to the entire ventral wall of the stomach and duodenum, three inoculations per site were performed. The total inoculated volume was 100 μ l, as for intrastriatal inoculation.

A number of parameters were monitored during the course of the 2-year study, including survival and clinical observations. At the end of the experiments (24 months post-injection), all monkeys were euthanized with pentobarbital overdose (150 mg/kg intravenously), followed by perfusion with room temperature 0.9% saline solution (containing 1% heparin) in accordance with accepted European Veterinary Medical Association guidelines. Brains were removed quickly after death. Each brain was then dissected along the midline and each hemisphere was divided into three parts. The left hemisphere was immediately freshly frozen by immersion in a cold isopentane bath at -50°C for at least 5 min and stored at -80°C for biochemical investigation. The right hemisphere was post-fixed for 1 week in 10 vol% tissue of 4% paraformaldehyde at 4°C , cryoprotected in two successive gradients of 20% then 30% sucrose in phosphate-buffered saline (PBS) before being frozen by immersion in a cold isopentane bath (-50°C) for at least 5 min and stored immediately at -80°C until sectioning. The thoracic vagus nerve was exposed by blunt dissection. Care was taken during the dissection not to distort the spatial relationship.

The thoracic vagus nerves were post-fixed, cryo-protected and frozen, as indicated above for the brain. The stomach and duodenum were removed and placed in a Sylgard[®]-coated Petri dishes containing fresh Hank's balanced salt solution (HBSS, Life Technologies). Then, tissue was stretched, pinned flat, and fixed for 3 h in a solution of PBS (Life Technologies) containing 4% paraformaldehyde (Sigma-Aldrich). Finally, tissue was washed three times with PBS and stored in a PBS solution containing 0.1% NaN_3 (Sigma-Aldrich) at 4°C . CSF and blood samples (plasma, serum, whole blood) for all 14 animals were taken before euthanasia. No samples were excluded from analysis in these studies.

Histopathological analysis of the brain

Extent of lesion

To assess the integrity of the nigrostriatal pathway, tyrosine hydroxylase (TH) immunohistochemistry was performed on SNpc and striatal sections. Briefly, sections from posterior level of the striatum and serial sections (1 in 12) corresponding to the whole SNpc were incubated with a rabbit monoclonal antibody raised against human TH (Abcam, ab137869, 1:1000) and with a mouse monoclonal antibody raised against human TH (Millipore, MAB318, 1:5000), respectively for 1 night at room temperature and revealed by an anti-mouse peroxidase EnVision[™] system (Dako, K400311) followed by 3,3'-diaminobenzidine (DAB) visualization. Free-floating SNpc sections were mounted on gelatinized slides, counterstained with 0.1% cresyl violet solution, dehydrated and cover-slipped, while striatal sections were mounted on gelatinized slides and cover-slipped. The extent of the lesion in the striatum was quantified by optical density (OD). Sections were scanned in an Epson expression 10000XL high resolution scanner and images were used in ImageJ open source software to compare the grey level in each region of interest: i.e. caudate nucleus and putamen. TH-positive SNpc cells were counted by stereology, blind with regard to the experimental condition, using a Leica DM6000B motorized microscope coupled with the Mercator software (ExploraNova). The SNpc was delineated for each slide and probes for stereological counting were applied to the map obtained (size of

probes was $100 \times 80 \mu\text{m}$ spaced by $600 \times 400 \mu\text{m}$). Each TH-positive cell with its nucleus included in the probe was counted. The optical fractionator method was finally used to estimate the total number of TH-positive cells in the SNpc of each monkey hemisphere. In addition, we measured Nissl cell count, the volume of SNpc, and the surface of TH-occupied in SNpc to characterize the pattern of dopaminergic loss in the SNpc.

α -Synuclein pathology

Synucleinopathy was assessed with a mouse monoclonal antibody raised against human α -synuclein (clone syn211, Thermo Scientific, MS1572, 1:1000) and phosphorylated α -synuclein (clone 11A5, Elan, 1:10 000) immunostaining as previously reported (Recasens *et al.*, 2014; Bourdenx *et al.*, 2015). Briefly, selected sections at two rostro-caudal levels were specifically identified and incubated in a same well to allow direct comparison of immunostaining intensity. Sections were incubated overnight at room temperature with the aforementioned antibodies. The following day, sections were incubated with anti-species peroxidase EnVision™ system (Dako) followed by DAB incubation. Sections were then mounted on gelatinized slides, dehydrated, counterstained if necessary with 0.1% cresyl violet and cover-slipped until further analysis. Grey level quantification or immunostaining-positive surface quantification in 20 brain regions (Fig. 2 and Supplementary Fig. 3) were performed as previously described (Bourdenx *et al.*, 2015). All analyses were evaluated evaluator-blinded.

Inflammation

Inflammatory processes in the striatum, entorhinal cortex and white matter of non-Lewy body and Lewy body-injected monkeys was measured by GFAP/S-100 (Dako, Z0334/Abnova, PAP11341) and Iba1 (Abcam, ab5076) immunohistochemistry. Striatal sections of all animals were incubated together overnight with a mix of rabbit antibodies raised against GFAP and S-100 for the astroglial staining (respective dilutions 1:2000 and 1:1000) and with goat anti-Iba1 antibody for the microglial staining (dilution 1:1000). These signals were revealed using the anti-species peroxidase EnVision system (Dako) followed by DAB incubation. Sections were mounted on slides, counterstained in 0.1% cresyl violet solution, dehydrated and cover-slipped. Sections stained by GFAP-S-100 were analysed at $\times 20$ magnification with a NanoZoomer (Hamamatsu) and the quantification of the GFAP-positive astrocytic reaction was estimated using an immunostaining-positive surface quantification at regional levels with the Mercator software (ExploraNova). Sections stained by Iba1 were used for the microglial morphology analysis through fractal dimension quantification based on microscopic acquisitions, as previously described (Soria *et al.*, 2017). All analyses were performed blinded to the researcher.

Histopathological analysis of the thoracic vagal nerve

Longitudinal $10 \mu\text{m}$ cryosections of the vagus nerve were made for each animal. Two representative sections by animal were used to assess synucleinopathy. All slides were incubated together with either a mouse monoclonal antibody raised against phosphorylated α -synuclein (clone 11A5, Elan, 1:10 000) or a

mouse monoclonal antibody against aggregated α -synuclein (clone 5G4, Millipore MABN389, 1:1000) and revealed by an anti-mouse peroxidase EnVision™ system followed by DAB visualization and counter-stained with 0.1% cresyl violet as described earlier for the brain sections. Slides were scanned with a high-resolution scanner (PanScan, 3D Histech) at $\times 20$ magnification and on five layers. The extended picture obtained was used to analyse the positive surface of the phosphorylated α -synuclein staining based on a selective colour threshold within the fibre or cell areas of the vagal nerve.

Histopathological analysis of the dorsal motor nucleus of the vagus

Coronal $50\text{-}\mu\text{m}$ serial cryosections of the dorsal motor nucleus of the vagus (dmnX) were made for each animal (1/6). Three adjacent series of sections were used by animal to assess choline acetyltransferase (ChAT) and synucleinopathy. Free floating sections were incubated with either a goat polyclonal antibody raised against ChAT (AB144P, Millipore, 1:1000), a mouse monoclonal antibody raised against human α -synuclein (clone syn211, Thermo Scientific, MS1572, 1:1000) or a mouse monoclonal antibody raised against phosphorylated α -synuclein (Abcam, ab51253, 1:5000), revealed by a specific anti-species peroxidase polymer detection system (anti-goat ImmPress Vector, MP7405 or anti-mouse/rabbit peroxidase EnVision™, Agilent K400111-2/K400311-2) followed by DAB visualization (Dako, K346811-2). Sections were then mounted on slides and counterstained with 0.1% cresyl violet as described earlier for the brain sections. All slides were scanned with a high-resolution scanner (PanScan, 3D Histech) at $\times 20$ magnification on five layers of $1 \mu\text{m}$ each. The extended picture obtained is used to illustrate the dmnX location (based on the ChAT signal) and the α -synuclein and phosphorylated α -synuclein staining within the dmnX.

Histopathological analysis of the enteric nervous system

Layers of tissue containing the myenteric plexus were separated by microdissection. Samples were permeabilized for 4 h in a 4% horse serum/PBS blocking buffer containing 0.5% Triton™ X-100 (Sigma-Aldrich), and incubated overnight at 4°C with the following primary antibodies diluted in the blocking buffer: mouse anti-Syn 1 (1:200; 610787, BD Bioscience), rabbit anti-Human NF200 (1:250; ab8135, Abcam), goat anti-human Sox10 (1:250; sc-17343, Santa Cruz Biotechnology), rabbit anti-Human Neuron specific enolase (NSE) (1:3000; 17437; Polysciences Inc.). Following incubation with primary antibodies, tissues were washed with PBS and incubated for 3 h at room temperature with a combination of donkey anti-mouse IgG conjugated to CY5 (1:500; 715-175-151, Jackson ImmunoResearch, Interchim), donkey anti-goat IgG conjugated to CY2 (1:500; FP-SA2110, Interchim) and donkey anti-rabbit IgG conjugated to CY3 (1:500; 711-165-152, Jackson ImmunoResearch, Interchim). Tissues were then washed with PBS and mounted with ProLong™ Gold antifade reagent (P36930, Thermo Fisher).

Biochemical analysis

Total protein extraction and quantification

Tissue patches ($n = 5$) of substantia nigra, putamen and caudate nucleus were extracted on ice using 100 μ l of RIPA buffer [50 mM Tris-HCl pH 7.4, 150 mM NaCl, 1.0% TritonTM X-100, 0.5% Na-deoxycholate, 0.1% sodium dodecyl sulphate (SDS)] with a protease inhibitor cocktail tablet (Complete Mini, Roche Diagnostics). Tissue from antrum and fundus were extracted on ice using 500 μ l SDS-urea 8%. In both cases, lysates were incubated on ice for 20 min then centrifuged at 14 000 rpm for 15 min at 4°C. The supernatants were collected and the total amount of protein in the lysates were determined by bicinchoninic acid (BCA) assay prior to storage at -80°C. Based on total protein concentrations calculated from the BCA assays, aliquots of tissue lysates corresponding to known amounts of total protein per dot were prepared for each animal in Laemmli buffer (Tris-HCl 25 mM pH = 6.8, glycerol 7.5%, SDS 1%, DTT 250 mM and bromophenol blue 0.05%) for dot-blotting experiments.

Dot-blot analysis of α -synuclein

This technique was performed as previously described (Recasens *et al.*, 2014; Bourdenx *et al.*, 2017). After heating at 100°C for 5 min, 20 μ g of protein extract was diluted in buffer (25 mM Tris-HCl, 200 mM glycine, 1% SDS) and filtered through either a nitrocellulose membrane or an acetate cellulose membrane (Bio-Rad, 0.2 μ m pore size). Membranes were then saturated in 5% dried skimmed milk in PBS and probed with antibodies against α -synuclein (syn211, 1:1000), both α -synuclein fibrils and α -synuclein oligomers (Syn-O1, 1:10 000) (kindly provided by Prof. Omar El-Agnaf) (Vaikath *et al.*, 2015; Helwig *et al.*, 2016). Appropriate secondary antibodies coupled to peroxidase were revealed using a Super Signal West Pico Chemiluminescent kit (Immobilon Western, Chemiluminescent HRP substrate, Millipore). Chemiluminescence images were acquired using the ChemiDocTM XRS+ system measurement (Bio-Rad). Signals per lane were quantified using ImageJ and a ratio of signal on loading per animal was performed and used in statistical analyses.

Sequential α -synuclein extraction and quantification

Tissue patches ($n = 10$) of posterior putamen were homogenized in Triton-X (TX) extraction buffer (50 mM Tris-base pH 7.6, 150 mM NaCl, 1% TritonTM X-100, 2 mM EDTA) containing protease and phosphatase inhibitors. The lysate was sonicated and then centrifuged (120 000g for 60 min at 4°C) and the supernatant was collected (TX soluble fraction). The pellet was then resuspended in SDS extraction buffer (50 mM Tris pH 7.6, 150 mM NaCl, 1% TritonTM X-100, 0.5% Na-deoxycholate, 1% SDS), sonicated, and centrifuged (120 000g for 60 min at 4°C) and the supernatant was collected (TX insoluble fraction). The total amount of protein in the lysates were determined by BCA prior to prepare aliquots for each animal in Laemmli buffer (Tris-HCl 25 mM pH 6.8, glycerol 7.5%, SDS 1%, DTT 250 mM and bromophenol blue 0.05%) for immunoblotting experiments. For immunoblotting, 20 μ g of protein was loaded per lane and separated on 12% SDS-PAGE; transferred to nitrocellulose membranes; and immunoblotted with mouse anti- α -synuclein (Syn211, 1:1000, Thermo Scientific) or anti-S129 phosphorylated α -synuclein (EP1536Y, 1:1000, Abcam). Anti-actin (1:5000, Sigma) was used to control equal loading. Appropriate secondary antibodies coupled to peroxidase were

revealed using a SuperSignalTM West Pico Chemiluminescent kit (Immobilon Western, Chemiluminescent HRP substrate, Millipore). Chemiluminescence images were acquired using the ChemiDocTM XRS+ system measurement (Bio-Rad). Signals per lane were quantified using ImageJ and a ratio of signal on loading per animal was performed and used for statistical analyses.

Human α -synuclein aggregation TR-FRET immunoassay

Time-resolved Förster's resonance energy transfer (TR-FRET)-based immunoassays were validated for total and oligomeric α -synuclein (Bidinosti *et al.*, 2012). Ten microlitres of brain and ENS samples were analysed for total α -synuclein quantification with the TR-FRET immunoassays kit against human α -synuclein aggregation kit (Cisbio, #6FASYPEG) according to the manufacturer's instructions.

Vagal nerve protein extraction

We used ~ 2 mm³ formalin-fixed tissue per animal. Protein was extracted using the Qproteome FFPE Tissue Kit (Qiagen), and then quantified using the Lowry method (Biorad RC DC Protein Assay Kit) following the manufacturer's instructions. Fifty micrograms of protein was used for dot-blotting experiments.

Measurement of α -synuclein in monkey biological fluid samples

Multi-Array 96-well plates (MesoScale Discovery) were coated with 30 μ l of 3 μ g/ml MJFR1 (Abcam) as capture antibody and incubated overnight at 4°C without shaking. The next day plates were washed three times with 150 μ l PBS-T [PBS (AppliChem) supplemented with 0.05% Tween-20 (Roth)] per well. Non-specific binding of proteins was prevented by incubation with 150 μ l of 1% bovine serum albumin (BSA) (SeraCare Life Sciences)/PBS-T/well for 1 h and shaking at 700 rpm. Calibrators (kindly provided by Prof. Omar El-Agnaf) were prepared from single use aliquots of α -synuclein (1 μ g/ml stored at -80°C until use) and ranged from 25 000 pg/ml to 6.1 pg/ml in serial 4-fold dilutions. BSA/PBS-T (1%) served as a blank. For the different specimens, the following dilutions were applied: 1 in 10 000 for whole blood and 1 in 8 for serum, plasma and CSF. All dilutions were prepared in 1% BSA/PBS-T. After washing the plates, 25 μ l calibrator solutions and diluted samples were applied to the wells and incubated as indicated above. Plates were washed again and 25 μ l Sulfo-TAG labelled Syn1 antibody (BD Biosciences) diluted to 1 μ g/ml in 1% BSA/PBS-T were applied to the wells as detection antibody. Sulfo-TAG labelling was done according to the manufacturer's instruction using MSD Sulfo-TAG NHS-Ester (MSD). Incubation was for 1 h at 700 rpm. Plates were washed, 150 μ l 2 \times Read Buffer (MSD) was applied and the plates were read on an MSD SectorImager 2400. Data analysis was performed using WorkBench software (MSD).

Statistical analysis

Statistical analyses were performed with GraphPad Prism 8.0 (GraphPad Software, Inc., San Diego, CA). For all experiments, comparisons among means were performed by using one-way ANOVA followed, if appropriate, by a pairwise comparison between means by Tukey's *post hoc* analysis. All values are

expressed as the mean \pm standard error of the mean (SEM). Correlations between variables were assessed with Spearman's correlation analysis, and we estimated effect size with Cohen's *d*. In all analyses, statistical significance was set at $P < 0.05$.

Data availability

The data supporting the findings of this study are available from the corresponding authors upon reasonable request.

Results

Here, we compare, in baboon monkeys ($n = 4\text{--}6$ per experimental group), the pathological consequences of either intra-striatal or enteric injection of Lewy body-enriched fractions containing pathological α -synuclein, purified from post-mortem Parkinson's disease patient brains. Lewy body-enriched fractions are composed (90%) of insoluble aggregated, detergent and proteinase K-resistant α -synuclein co-localizing with the β -sheet-rich structures binding dye thioflavin S (Bourdenx *et al.*, 2019).

Two years after administration, Lewy body-injected monkeys displayed a loss of dopaminergic neurons and fibres regardless of the injection site (Fig. 1A–D) compared to age-matched control monkeys as previously reported (Recasens *et al.*, 2014; Bourdenx *et al.*, 2019). Injection of Lewy body-enriched fractions in the ENS led to striatal dopaminergic loss, to the same extent as in striatum-injected animals (Fig. 1A–D). Both CNS and ENS injections resulted in loss of TH immunoreactivity in the SNpc and loss of striatal dopaminergic terminals; but these lesions remained below the threshold for the appearance of parkinsonian symptoms (Bezard *et al.*, 2001). There was a relatively modest degeneration of the nigrostriatal pathway in ENS-injected animals compared to striatum-injected animals, suggesting that the Lewy body-induced neurodegenerative process might have been ongoing and progressing more slowly in the former, corresponding to an early/premotor stage of Parkinson's disease (Supplementary Fig. 1). At 2 years, apart from an increased Iba1 immunoreactivity in the entorhinal cortex of the striatum-injected animals, no gross astrogliosis and microgliosis was observed in the CNS of Lewy body-injected animals (Supplementary Fig. 2). To evaluate whether Lewy body-induced neurodegeneration was associated with α -synuclein pathology, we quantified the expression levels of α -synuclein in 18 brain regions (Fig. 2A and Supplementary Fig. 3). We found mild differences in α -synuclein immunolabelling after both striatum and ENS injections compared to age-matched control monkeys, except for the posterior part of the putamen, where a significant increase in α -synuclein signal was observed in both experimental groups. By contrast, the pathogenic form of α -synuclein, i.e. S129 phosphorylated α -synuclein, accumulated differently in the Lewy body-injected animal groups (Fig. 2A). Striatum-injected animals exhibited a marked accumulation in the basal ganglia and various cerebral cortical areas, while accumulation was overall milder in ENS-injected monkeys (Fig. 2A–C). We

then measured the content of α -synuclein aggregates using TR-FRET immunoassay and observed no differences in the three brain regions investigated in striatum-injected animals (Supplementary Fig. 4A). However, sequential α -synuclein extraction of brain patches revealed overall increased Triton-soluble and -insoluble monomeric and high molecular weight forms of total and S129 phosphorylated α -synuclein in the posterior putamen of striatum-injected animals (Supplementary Fig. 5). Using Syn-O1, an antibody specific for α -synuclein fibrils and oligomers (Vaikath *et al.*, 2015), we detected oligomeric and fibrillar forms of the protein in nigrostriatal regions in some Lewy body-injected animals (Supplementary Fig. 6), corroborating the biochemistry results. As a whole, these findings suggest that enteric injection of Lewy body-enriched fractions might induce α -synuclein pathology throughout the nigrostriatal tract, similar to that observed after striatal injection and confirm that α -synuclein pathology is present in the CNS independently of the site of injection.

To assess whether the pathogenic effects of Parkinson's disease-derived Lewy bodies extracts could also be observed throughout the ENS, we evaluated the presence of α -synucleinopathy in the duodenum, close to the site of injection, and at a distance from the injection (in the fundus and the antrum). We first determined α -synuclein expression patterns in the monkey ENS, where we found that native α -synuclein is abundantly expressed in monkey enteric neurons, as shown by co-localization of α -synuclein with pan-neuronal markers (Supplementary Fig. 7). Then, using confocal microscopy, we observed a significant increase ($\sim 600\%$) in α -synuclein immunoreactivity in enteric neurons [i.e. neuron-specific enolase (NSE)-positive cells] in ENS-injected monkeys compared to age-matched controls (Fig. 3A and B). Even more interestingly, levels of α -synuclein accumulation in NSE-positive cells were also significantly increased in the striatum-injected group (Fig. 3A and B). The presence of α -synuclein aggregates in the fundus and antrum was further assessed. While TR-FRET immunoassay showed no changes in experimental groups (Supplementary Fig. 4B), stomach samples from striatum- and ENS-injected animals contained oligomeric forms of α -synuclein as revealed by dot-blot assay using Syn-1 and Syn-O1 antibodies (Supplementary Fig. 8). These results confirm the presence of an enteric α -synuclein pathology after both intra-ENS or intra-striatal injections. Interestingly, there was a significant negative correlation between the intensity of α -synuclein immunoreactivity in enteric neurons and the TH immunoreactivity in the putamen (Fig. 3C) and in the SNpc (Fig. 3D), implying that a high α -synuclein level in enteric neurons correlated with the progressive destruction of the nigrostriatal pathway. These findings suggest that α -synuclein level in enteric neurons may reflect the severity of pathological changes occurring in the prodromal phase of patients with Parkinson's disease. This notion is supported by the findings of a study that the progressive loss of dopamine transporter in the caudate nucleus correlated significantly with progressive constipation symptoms (Hinkle *et al.*, 2018), raising the possibility that striatal

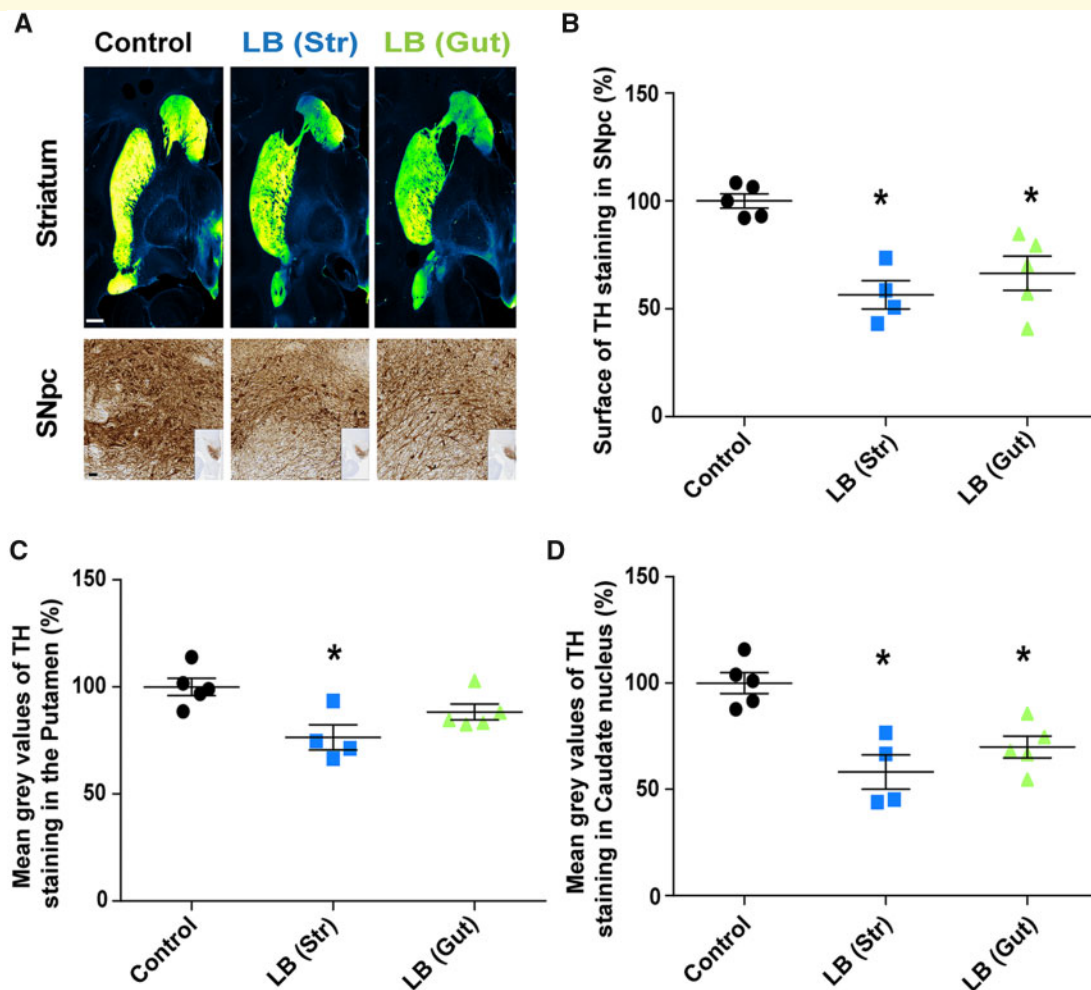


Figure 1 Injection of Lewy bodies from patients with Parkinson's disease into striatum or ENS (gut) induces nigrostriatal neurodegeneration and synucleinopathy in the brain of baboon monkeys 2 years after administration. **(A)** TH staining at striatum and SNpc levels. A green fire blue LUT (lookup table) was used to enhance contrast and highlight the difference between controls ($n = 5$), and monkeys injected with Lewy bodies either into the striatum ($n = 4$) or gut ($n = 5$). Scale bars = 5 mm (striatum) and 10 μm (SNpc). **(B)** Scatter plot of TH immunostaining in SNpc. $F(2,11) = 13.42$, $P = 0.0011$. Control versus striatum: $P = 0.0014$; control versus gut: $P = 0.0060$; striatum versus gut: $P = 0.5320$. **(C and D)** Scatter plots of mean grey values of striatal TH immunoreactivity in the putamen [$F(2,11) = 6.571$, $P = 0.0133$; control versus striatum: $P = 0.0104$; control versus gut: $P = 0.1809$; striatum versus gut: $P = 0.2103$] **(C)** and in the caudate nucleus [$F(2,11) = 13.26$, $P = 0.0012$; control versus striatum: $P = 0.0013$; control versus gut: $P = 0.0087$; striatum versus gut: $P = 0.3829$] **(D)** in controls, and monkeys injected with Lewy bodies either into the striatum or gut. The horizontal line indicates the average value per group \pm SEM. Each data point represents one control monkey (black), and monkeys injected with Lewy bodies either into the striatum (blue) or the gut (green). Comparisons were made using one-way ANOVA and Tukey's correction for multiple comparison. * $P < 0.05$ compared to control animals. LB = Lewy body.

dopaminergic denervation may have an instrumental role in the development of gastrointestinal dysfunction in Parkinson's disease (Borghammer, 2018). These results indicate that both striatal and ENS injections of Lewy body-enriched fractions can induce α -synuclein pathology in the ENS. We have, thus, demonstrated the bidirectional long-distance propagation of α -synuclein pathology between the CNS and the ENS in the non-human primate.

To investigate the precise route underlying such propagation, we evaluated the presence of phosphorylated α -synuclein in the vagus nerve in Lewy body-injected animals compared to controls (Fig. 4A). No significant difference in

S129 phosphorylated α -synuclein immunoreactivity was observed in the vagus nerve in Lewy body-injected monkeys compared to age-matched controls (Fig. 4B and C). The level of S129 phosphorylated α -synuclein in either the vagal nerve fibres (Fig. 4D) or the vagal cells (Fig. 4E) did not correlate with the α -synuclein immunoreactivity in enteric neurons and no increase in aggregated α -synuclein was observed in the vagus nerve of Lewy body-injected monkeys (Supplementary Fig. 9). We next examined the pathological features of the α -synuclein and S129 phosphorylated α -synuclein immunostaining in the dmNX. We showed that ChAT-positive neurons of the dmNX from non-injected animals

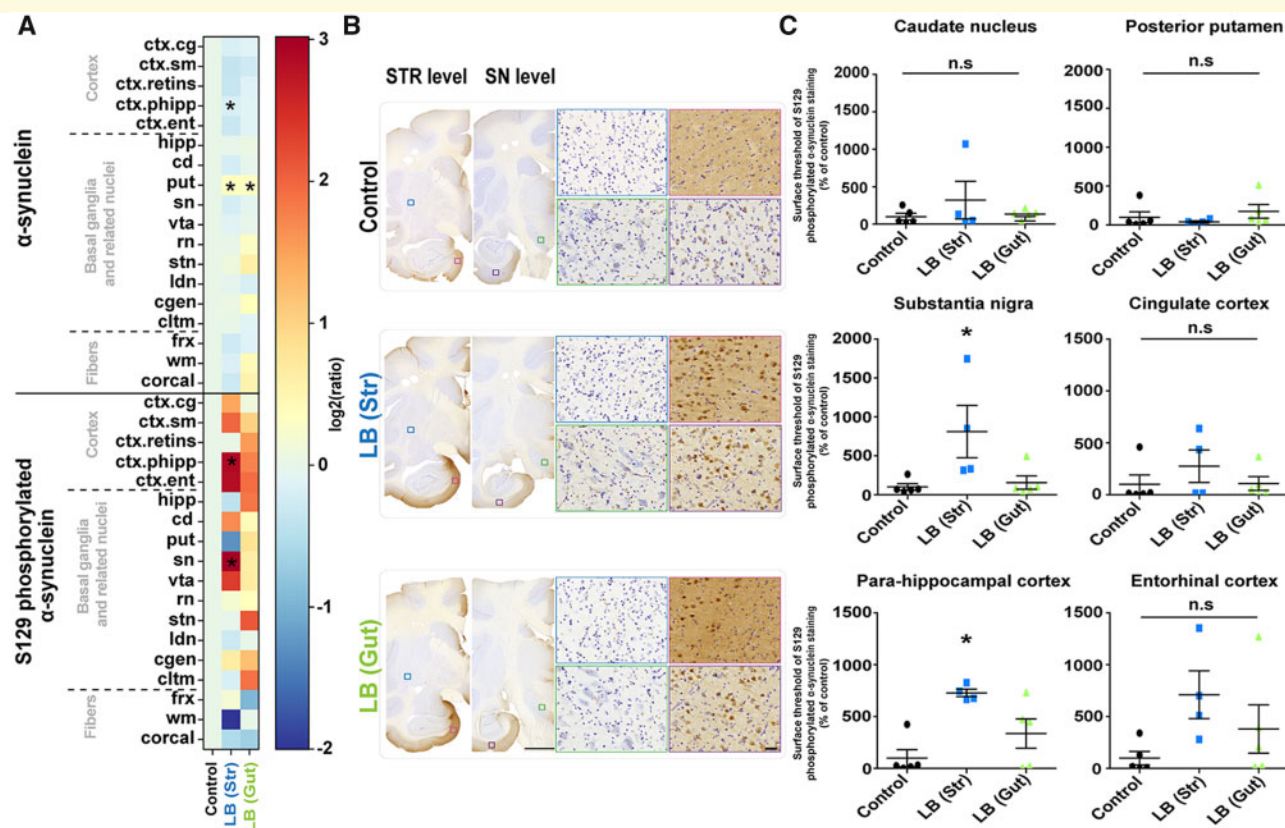
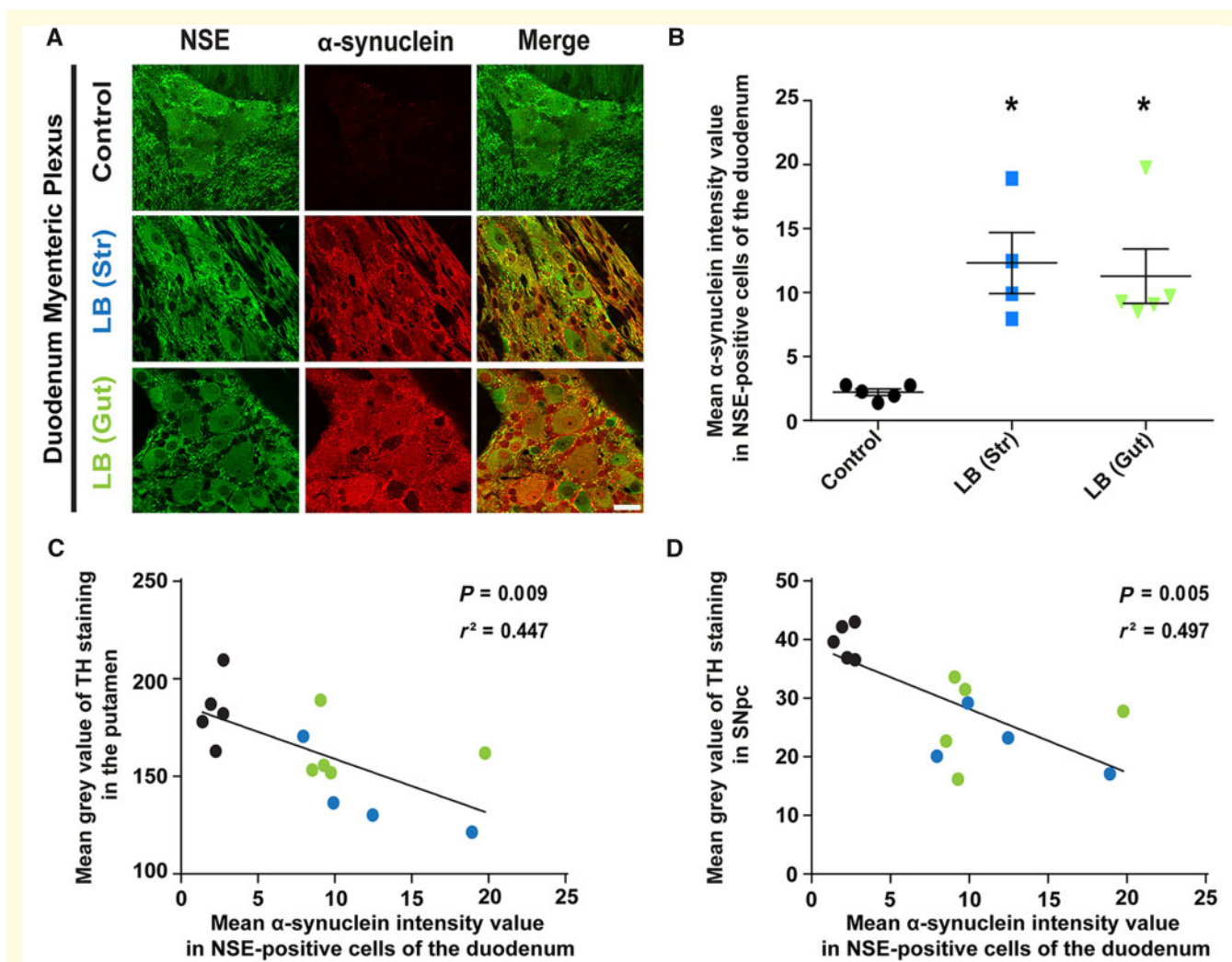


Figure 2 Lewy bodies injection into striatum or ENS (gut) induces a mild-to-moderate specific pattern of S129 phosphorylated α -synuclein levels in the brain of baboon monkeys. **(A)** Heat map representing the surface threshold of α -synuclein and S129 phosphorylated α -synuclein immunostaining intensity in the brain of control, and monkeys injected with Lewy bodies either into the striatum (Str) or gut (Gut). The heat maps show all brain regions measured and are organized according to cortical, basal ganglia and subcortical-related structure classification. From top to bottom: cingulate cortex (ctx.cg), sensorimotor cortex (ctx.sm), retro-insular cortex (ctx.retins), parahippocampal cortex (ctx.phipp), entorhinal cortex (ctx.ent), hippocampus (hipp), caudate nucleus (cd), putamen (put), substantia nigra (sn), ventral tegmental area (vta), red nucleus (rn), subthalamic nucleus (stn), lateral dorsal nucleus (ldn), lateral geniculate nucleus (cgen), claustrum (cltm), fornix (frx), white matter (wm), and corpus callosum (corcal). The colour bars represent the \log_2 value of the ratio of each brain region. Comparisons were made using one-way ANOVA and Tukey's correction for multiple comparisons. * $P < 0.05$ compared to control animals. **(B)** Representative coronal brain sections of endogenous α -synuclein immunostaining (left) and illustrative photomicrographs of endogenous α -synuclein in the putamen (blue square), in the SNpc (SN) (green square), in the entorhinal cortex (pink square) and in the parahippocampal cortex (purple square) in controls, and monkeys injected with Lewy bodies either into the striatum or gut. Scale bars = 5 mm (left, sections) and 40 μ m (right, insets). **(C)** Scatter plots of S129 phosphorylated α -synuclein immunostaining expressed in percentage of control group in the caudate nucleus [$F(2,11) = 0.8311$, $P = 0.4612$; control versus striatum: $P = 0.4681$; control versus gut: $P = 0.9786$; striatum versus gut: $P = 0.5743$]; in the posterior putamen [$F(2,11) = 0.8710$, $P = 0.4455$; control versus striatum: $P = 0.8379$; control versus gut: $P = 0.7223$; striatum versus gut: $P = 0.4206$]; in the substantia nigra [$F(2,11) = 4.808$, $P = 0.0316$; control versus striatum: $P = 0.0396$; control versus gut: $P = 0.9699$; striatum versus gut: $P = 0.0578$]; in the cingulate cortex [$F(2,11) = 0.8468$, $P = 0.4549$; control versus striatum: $P = 0.4918$; control versus gut: $P = 0.9981$; striatum versus gut: $P = 0.5226$]; in the parahippocampal cortex [$F(2,11) = 8.968$, $P = 0.0049$; control versus striatum: $P = 0.0038$; control versus gut: $P = 0.2555$; striatum versus gut: $P = 0.0558$] and in the entorhinal cortex [$F(2,11) = 2.526$, $P = 0.1251$; control versus striatum: $P = 0.1067$; control versus gut: $P = 0.5358$; striatum versus gut: $P = 0.4698$] in controls, and monkeys injected with Lewy bodies either into the striatum or gut. The horizontal line indicates the average value per group \pm SEM. Each data point represents one control monkey (black), and monkeys injected with Lewy bodies injected into either the striatum (blue) or the gut (green). Comparisons were made using one-way ANOVA and Tukey's correction for multiple comparison. * $P < 0.05$ compared to control animals. LB = Lewy body; n.s. = not significant.

contain α -synuclein and phosphorylated- α -synuclein (Fig. 5). However, injection of Lewy bodies into the striatum or into the ENS did not induce synucleinopathy in the dmX (Fig. 5).

Although further experiments in vagotomized animals will be required, our results indicate that α -synuclein

pathological lesions were not found in the vagal nerve in our experimental setting. The fact that α -synuclein can also be detected in several body fluids (El-Agnaf et al., 2003), logically led us to measure the α -synuclein concentration in monkey blood, which was preferentially chosen to avoid concerns about haemolysis. We observed a significantly



higher concentration of α -synuclein in whole blood (Fig. 4F) from the ENS-injected monkeys than in the controls. A similar observation was made in the serum of striatum-injected monkeys (Fig. 4G). No significant difference was observed in the plasma (Fig. 4H) or in the CSF (Fig. 4I). Interestingly, the α -synuclein concentrations in whole blood (Fig. 4J) and in plasma (Fig. 4K) were positively correlated with α -synuclein immunoreactivity in enteric neurons. These observations suggest that circulating levels of α -synuclein could reflect the initiation of synucleinopathy in the ENS or the

brain and strengthen its predictive role as a biomarker. Whether these elevated levels of circulating α -synuclein solely reflect the status of the pathology or contribute to the disease itself as a route propagation or transmission remain to be fully addressed.

Discussion

Here, our data provide evidence that both striatal and ENS injections of Lewy body-enriched fractions in baboon

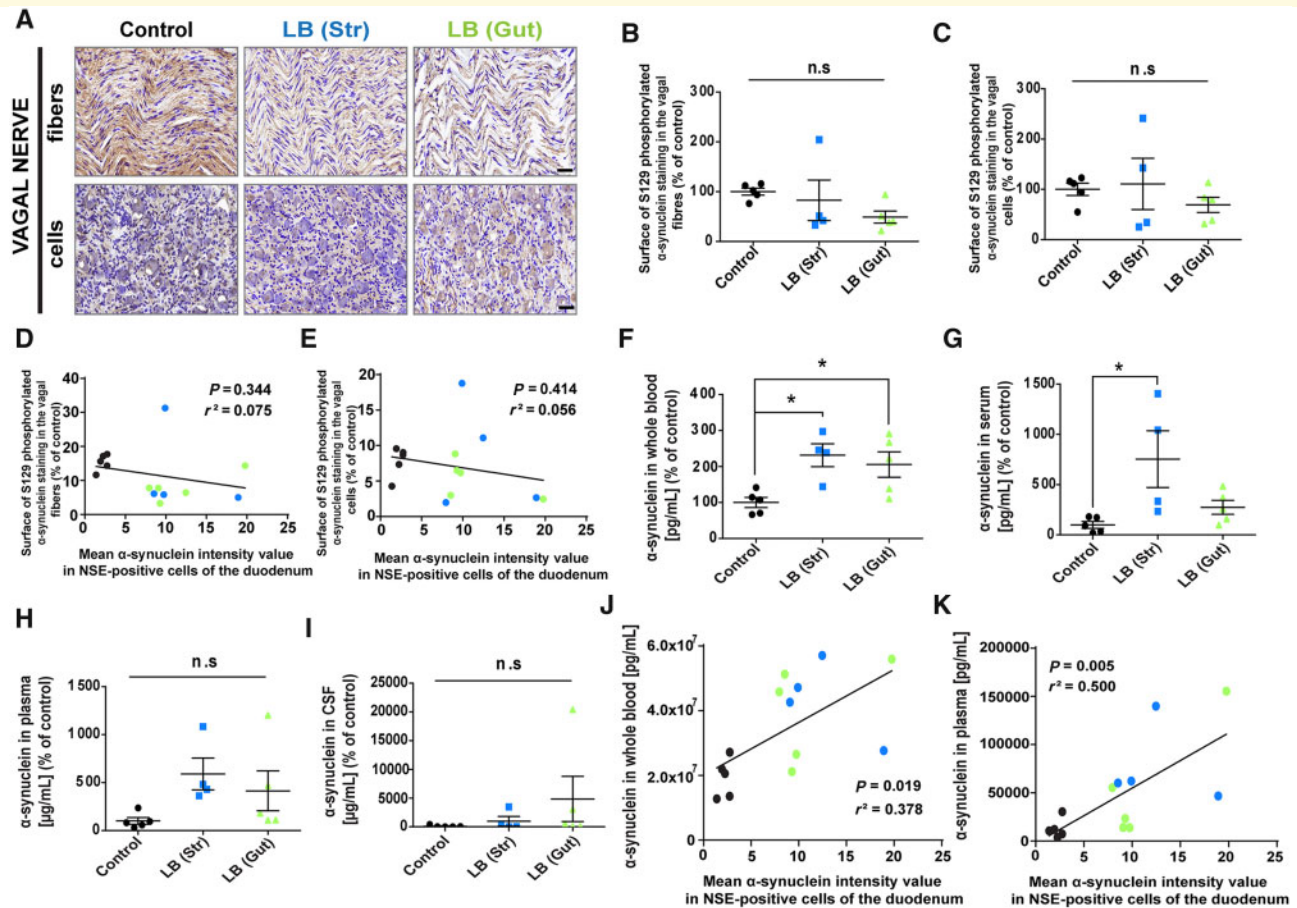


Figure 4 Routes of propagation of α -synuclein between the CNS and ENS. (A) Representative images of S129 phosphorylated α -synuclein immunostaining into the fibres (top) and the cells (bottom) of the vagal nerve in controls, and monkeys injected with Lewy bodies either into the striatum (Str) or gut (Gut). Scale bar = 40 μ m. (B and C) Scatter plot of S129 phosphorylated α -synuclein immunostaining (B) in the vagal fibres [$F(2,11) = 1.545, P = 0.2562$; control versus striatum: $P = 0.8445$; control versus gut: $P = 0.2367$; striatum versus gut: $P = 0.5474$] and (C) in the vagal cells [$F(2,11) = 0.6148, P = 0.5583$; control versus striatum: $P = 0.9595$; control versus gut: $P = 0.7000$; striatum versus gut: $P = 0.5650$]. The horizontal line indicates the average value per group \pm SEM. Comparisons were made using one-way ANOVA and Tukey's correction for multiple comparison. * $P < 0.05$ compared to control animals. (D and E) Linear regression between the mean α -synuclein immunostaining in NSE-positive cells of the duodenum and the surface occupied by the S129 phosphorylated α -synuclein immunostaining (D) in the vagal fibres [$F(1,12) = 0.9714, P = 0.3438, r^2 = 0.0749$] and (E) in the vagal cells [$F(1,12) = 0.7163, P = 0.4139, r^2 = 0.0563$] for controls, and monkeys injected with Lewy bodies either into the striatum or gut. (F–I) Scatter plot of α -synuclein concentration (F) in whole blood [$F(2,11) = 6.086, P = 0.0166$; control versus striatum: $P = 0.0211$; control versus gut: $P = 0.0476$; striatum versus gut: $P = 0.8077$]; (G) in the serum [$F(2,11) = 5.099, P = 0.0271$; control versus striatum: $P = 0.0242$; control versus gut: $P = 0.6610$; striatum versus gut: $P = 0.0995$]; (H) in the plasma [$F(2,11) = 2.521, P = 0.1255$; control versus striatum: $P = 0.1179$; control versus gut: $P = 0.3345$; striatum versus gut: $P = 0.7198$]; and (I) in the CSF [$F(2,11) = 1.092, P = 0.3694$; control versus striatum: $P = 0.9686$; control versus gut: $P = 0.3745$; striatum versus gut: $P = 0.5461$]. The horizontal line indicates the average value per group \pm SEM. Comparisons were made using one-way ANOVA and Tukey's correction for multiple comparison. * $P < 0.05$ compared to control animals. (J and K) Linear regression between the mean α -synuclein immunostaining in NSE-positive cells of the duodenum and the α -synuclein concentration (J) in the whole blood [$F(1,12) = 7.289, P = 0.0193, r^2 = 0.3779$] and (K) in the plasma [$F(1,12) = 11.98, P = 0.0047, r^2 = 0.4996$], for controls, and Lewy body-injected monkeys either into the striatum or in the gut. Each data point in B–K represents one control monkey (black), and monkeys injected with Lewy bodies either into the striatum (blue) or in the gut (green). Spearman r and P -values are displayed on the graph. LB = Lewy body.

monkeys induce nigrostriatal degeneration associated with α -synuclein pathology in both the CNS and the ENS (Supplementary Table 1 features all raw data). Thus, our results reveal the existence of a bidirectional route of propagation of α -synuclein between the CNS and the ENS (Fig. 6) and within the ENS (i.e. stomach to duodenum). Our results do not support the hypothesis of a transmission of α -

synuclein pathology through the vagus nerve and then the dmX (as can be observed at this time point). Instead, our results suggest a possible systemic mechanism, in which the general circulation would act as a route for long-distance bidirectional transmission of endogenous α -synuclein between the ENS and the CNS. These findings are in agreement with two independent recent reports showing gut-to-brain

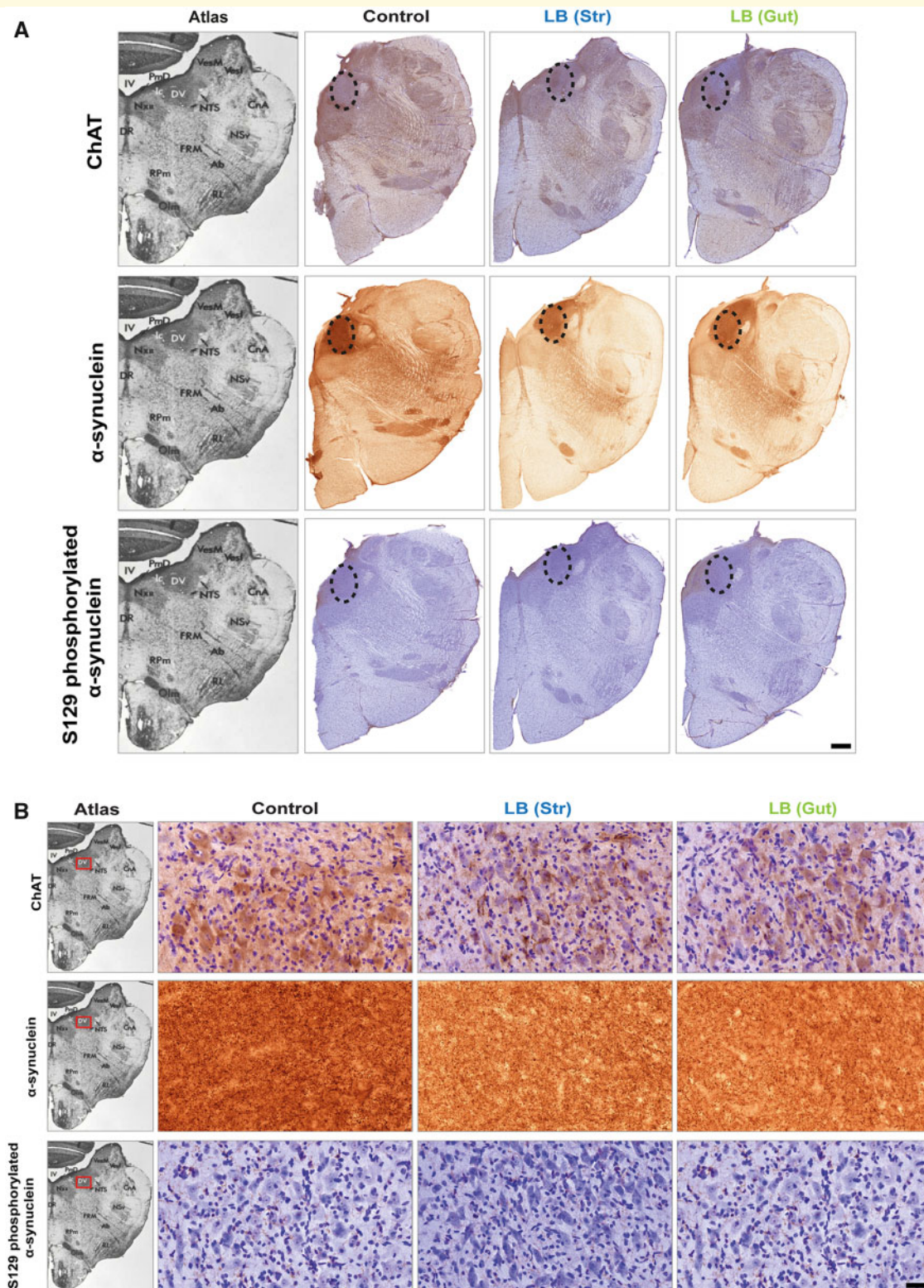


Figure 5 Injection of Lewy bodies into striatum or ENS (gut) does not induce synucleinopathy in the dmX in baboon monkeys.

(A) Illustration adapted from the baboon brain stereotaxic atlas of Davis and Huffman (1968) depicting the dmX in a cresyl-violet-stained brain section (left) and representative coronal brain section of ChAT, endogenous α -synuclein and S129 phosphorylated α -synuclein immunostaining (right) in the dmX. Scale bar = 2 mm. **(B)** Schematic (left) and representative images of immunohistochemical staining for ChAT, α -synuclein, S129 phosphorylated α -synuclein (right) in the dmX, based on the stereotaxic atlas of the baboon brain of Davis and Huffman (1968). Scale bars = 40 μ m. Ab = nucleus ambiguus; CnA = accessory cuneate nucleus; DR = dorsal raphe nucleus; DV = dorsal nucleus of vagus nerve; FRM = reticular formation; IV = fourth ventricle; Ic = intercalated nucleus; NSv = spinal trigeminal nucleus; NTS = solitary nucleus; Olm = medial accessory olivary nucleus; PmD = median dorsal nucleus; RL = lateral reticular nucleus; Rpm = median reticular nucleus; Vesl = inferior vestibular nucleus; VesM = median vestibular nucleus.

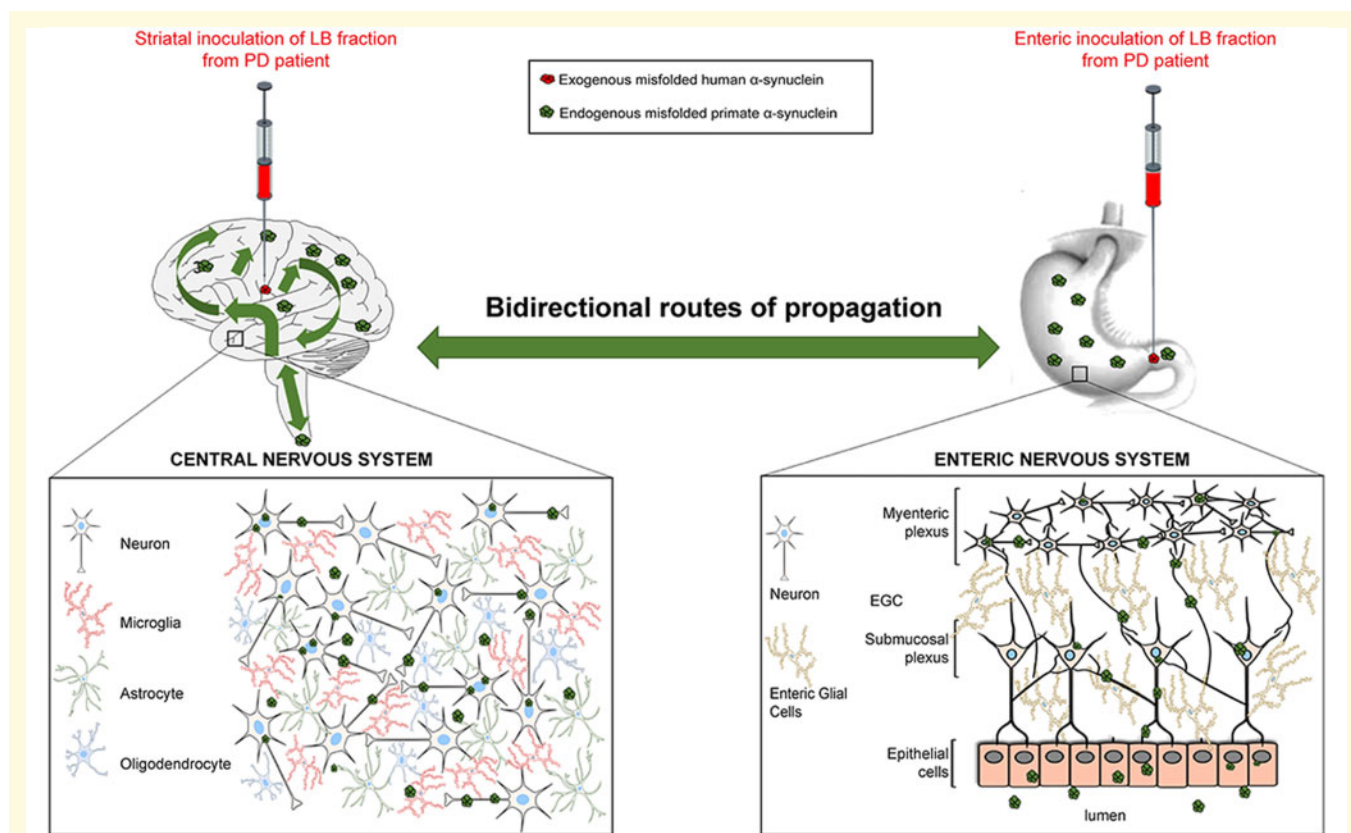


Figure 6 Schematic illustration of the bidirectional propagation of α -synuclein pathology between the CNS and the ENS.

Injection of Lewy body-enriched fractions from patients with Parkinson's disease (PD) into the duodenum induced the initiation of α -synuclein pathogenicity locally in the ENS before propagating anterogradely towards the CNS. Conversely, injection of Lewy body-enriched fractions from patients with Parkinson's disease into the striatum induced the initiation of the α -synuclein pathogenicity locally in the CNS before propagating retrogradely towards the ENS. Thus, the α -synuclein pathology propagated in a bidirectional manner between the CNS and the ENS before spreading in each nervous system through cell-to-cell transmission. EGC = enteric glial cells; LB = Lewy body.

transmission of Parkinson's disease pathology in two distinct rodent models based on the injection of α -synuclein pre-formed fibrils into the muscularis layer of the duodenum and pylorus in mice (Kim *et al.*, 2019) and into the wall of the duodenum in transgenic rats overexpressing human α -synuclein (Van Den Berge *et al.*, 2019). The latter study also proposed an alternative route of α -synuclein spreading through the coeliac ganglia and independent of the vagal nerve (Van Den Berge *et al.*, 2019).

Overall, the literature is consistent on the spread of α -synuclein pathology rostrally and the present study confirms this observation in non-human primates. However, our study also shows that α -synuclein can spread caudally. The route of propagation needs to be further elucidated. It is likely that the answer depends of the animal model, the inoculum, the species and the time post-injection. In this context, our study provides invaluable primate data exploring the role of the gut-brain axis in the initiation and propagation of Parkinson's disease pathology and should open the door to the development and testing of new therapeutic approaches aimed at interfering with the development of sporadic Parkinson's disease.

Acknowledgements

The authors wish to express their gratitude to Prof Alan R. Crossman (University of Manchester, UK) for his comments and for his advice on English grammar. The authors thank Carmen Lagares Martínez (Head, Veterinary Service, University of Murcia) for administrative assistance; Maria Fermina Ros Romero and Josefa Martínez Rabadán (University of Murcia) for veterinary and husbandry support; Ana Luisa Gil, Lorena Cuenca Bermejo and Ignacio Mascarell from the Clinical and Experimental Neuroscience group (University of Murcia) for their technical help with various parts of the *in vivo* part of these complex experiments. We would like to thank Philippe Hantraye (MIRcen) for providing baboon stereotactic frame.

Funding

The University of Bordeaux and the Centre National de la Recherche Scientifique provided infrastructural support. This work was supported by a grant from the Michael J Fox Foundation (Project Grant No. 2013-8499), Fundacion de

Investigacion HM Hospitales (Madrid, Spain), the Fundación Séneca (Project Grant No: FS19540/PI/14), the TARGET PD ANR grant and The Simone and Cino Del Duca Prize from French Academy of Sciences. M.B. and M.L.A. were supported by grants from Ministère de l'Enseignement Supérieur et de la Recherche fellowship and the France Parkinson Foundation. A.P. and P.D. were supported by grants from CECAP (comité d'entente et de coordination des associations de parkinsoniens) and 'Parkinsoniens de Vendée'. J.A.O. and I.T.D. were funded by MINECO/AEI/FEDER-UE (SAF2015-67239-P). The help of the Bordeaux Imaging Center, part of the national infrastructure France BioImaging, granted by ANR-10INBS-04-0, is acknowledged. The Human α -Synuclein aggregation TR-FRET immunoassay was done in the Biochemistry and Biophysics Platform of the Bordeaux Neurocampus at the Bordeaux University funded by the LABEX BRAIN (ANR-10-LABX-43) with the help of Y. Rufin. The samples were obtained from the Brain Bank GIE NeuroCEB (BRIF number 0033-00011), funded by the patients' associations France Alzheimer, France Parkinson, ARSEP, and 'Connaître les Syndromes Cérébelleux' to which we express our gratitude.

Competing interests

E.B. is a director and a shareholder of Motac Holdings Ltd. All other authors report no competing interests.

Supplementary material

Supplementary material is available at *Brain* online.

References

- Ahmed M, Berthet A, Bychkov E, Porras G, Li Q, Bioulac B, et al. Lentiviral overexpression of GRK6 alleviates L-dopa-induced dyskinesia in experimental Parkinson's disease. *Sci Transl Med* 2010; 2: 28ra.
- Beach TG, Adler CH, Sue LI, Vedders L, Lue L, White III CL, et al. Multi-organ distribution of phosphorylated alpha-synuclein histopathology in subjects with Lewy body disorders. *Acta Neuropathol* 2010; 119: 689–702.
- Bezard E, Dovero S, Prunier C, Ravenscroft P, Chalon S, Guilloteau D, et al. Relationship between the appearance of symptoms and the level of nigrostriatal degeneration in a progressive 1-methyl-4-phenyl-1,2,3,6-tetrahydropyridine-lesioned macaque model of Parkinson's disease. *J Neurosci* 2001; 21: 6853–61.
- Bidinosti M, Shimshek DR, Mollenhauer B, Marcellin D, Schweizer T, Lotz GP, et al. Novel one-step immunoassays to quantify alpha-synuclein: applications for biomarker development and high-throughput screening. *J Biol Chem* 2012; 287: 33691–705.
- Borghammer P. Is constipation in Parkinson's disease caused by gut or brain pathology? *Parkinsonism Relat Disord* 2018; 55: 6–7.
- Bourdenx M, Dovero S, Engeln M, Bido S, Bastide MF, Duthiel N, et al. Lack of additive role of ageing in nigrostriatal neurodegeneration triggered by alpha-synuclein overexpression. *Acta Neuropathol Commun* 2015; 3: 46.
- Bourdenx M, Koulakiotis NS, Sanoudou D, Bezard E, Dehay B, Tsaropoulos A. Protein aggregation and neurodegeneration in prototypical neurodegenerative diseases: examples of amyloidopathies, tauopathies and synucleinopathies. *Prog Neurobiol* 2017; 155: 171–93.
- Bourdenx M, Nioche A, Dovero S, Arotcarena ML, Camus S, Porras G, et al. Identification of distinct pathological signatures induced by patient-derived α -synuclein structures in non-human primates. *bioRxiv* 825216; doi:10.1101/825216 2019.
- Braak H, de Vos RA, Bohl J, Del Tredici K. Gastric alpha-synuclein immunoreactive inclusions in Meissner's and Auerbach's plexuses in cases staged for Parkinson's disease-related brain pathology. *Neurosci Lett* 2006; 396: 67–72.
- Braak H, Del Tredici K, Rub U, de Vos RA, Jansen Steur EN, Braak E. Staging of brain pathology related to sporadic Parkinson's disease. *Neurobiol Aging* 2003; 24: 197–211.
- Davis R, Huffman RD. A stereotaxic atlas of the brain of the baboon (papio). Austin: University of Texas Press; 1968.
- Edwards LL, Quigley EM, Pfeiffer RF. Gastrointestinal dysfunction in Parkinson's disease: frequency and pathophysiology. *Neurology* 1992; 42: 726–32.
- El-Agnaf OM, Salem SA, Paleologou KE, Cooper LJ, Fullwood NJ, Gibson MJ, et al. Alpha-synuclein implicated in Parkinson's disease is present in extracellular biological fluids, including human plasma. *FASEB J* 2003; 17: 1945–7.
- Fasano S, Bezard E, D'Antoni A, Francardo V, Indrigo M, Qin L, et al. Inhibition of Ras-guanine nucleotide-releasing factor 1 (Ras-GRF1) signaling in the striatum reverts motor symptoms associated with L-dopa-induced dyskinesia. *Proc Natl Acad Sci U S A* 2010; 107: 21824–9.
- Helwig M, Klinkenberg M, Rusconi R, Musgrove RE, Majbour NK, El-Agnaf OM, et al. Brain propagation of transduced alpha-synuclein involves non-fibrillar protein species and is enhanced in alpha-synuclein null mice. *Brain* 2016; 139: 856–70.
- Hinkle JT, Perezko K, Mills KA, Mari Z, Butala A, Dawson TM, et al. Dopamine transporter availability reflects gastrointestinal dysautonomia in early Parkinson disease. *Parkinsonism Relat Disord* 2018; 55: 8–14.
- Holmqvist S, Chutna O, Bousset L, Aldrin-Kirk P, Li W, Bjorklund T, et al. Direct evidence of Parkinson pathology spread from the gastrointestinal tract to the brain in rats. *Acta Neuropathol* 2014; 128: 805–20.
- Kim S, Kwon SH, Kam TI, Panicker N, Karuppagounder SS, Lee S, et al. Transneuronal propagation of pathologic alpha-synuclein from the gut to the brain models Parkinson's disease. *Neuron* 2019; 103: 627–41 e7.
- Knudsen K, Fedorova TD, Bekker AC, Iversen P, Ostergaard K, Krogh K, et al. Objective colonic dysfunction is far more prevalent than subjective constipation in Parkinson's disease: a colon transit and volume study. *J Parkinsons Dis* 2017; 7: 359–67.
- Lionnet A, Leclair-Visonneau L, Neunlist M, Murayama S, Takao M, Adler CH, et al. Does Parkinson's disease start in the gut? *Acta Neuropathol* 2018; 135: 1–12.
- Manfredsson FP, Luk KC, Benskey MJ, Gezer A, Garcia J, Kuhn NC, et al. Induction of alpha-synuclein pathology in the enteric nervous system of the rat and non-human primate results in gastrointestinal dysmotility and transient CNS pathology. *Neurobiol Dis* 2018; 112: 106–18.
- Miwa H, Kubo T, Suzuki A, Kondo T. Intra-gastric proteasome inhibition induces alpha-synuclein-immunopositive aggregations in neurons in the dorsal motor nucleus of the vagus in rats. *Neurosci Lett* 2006; 401: 146–9.
- Porras G, Berthet A, Dehay B, Li Q, Ladepeche L, Normand E, et al. PSD-95 expression controls L-DOPA dyskinesia through dopamine D1 receptor trafficking. *J Clin Invest* 2012; 122: 3977–89.
- Recasens A, Dehay B, Bove J, Carballo-Carbajal I, Dovero S, Perez-Villalba A, et al. Lewy body extracts from Parkinson disease brains trigger alpha-synuclein pathology and neurodegeneration in mice and monkeys. *Ann Neurol* 2014; 75: 351–62.

- Soria FN, Engeln M, Martinez-Vicente M, Glangetas C, López-González MJ, Dovero S, et al. Glucocerebrosidase deficiency in dopaminergic neurons induces microglial activation without neurodegeneration. *Hum Mol Genet* 2017; 26: 2603–15.
- Uemura N, Yagi H, Uemura MT, Hatanaka Y, Yamakado H, Takahashi R. Inoculation of alpha-synuclein preformed fibrils into the mouse gastrointestinal tract induces Lewy body-like aggregates in the brainstem via the vagus nerve. *Mol Neurodegener* 2018; 13: 21.
- Ulusoy A, Phillips RJ, Helwig M, Klinkenberg M, Powley TL, Di Monte DA. Brain-to-stomach transfer of alpha-synuclein via vagal preganglionic projections. *Acta Neuropathol* 2017; 133: 381–93.
- Ulusoy A, Rusconi R, Perez-Revuelta BI, Musgrove RE, Helwig M, Winzen-Reichert B, et al. Caudo-rostral brain spreading of alpha-synuclein through vagal connections. *EMBO Mol Med* 2013; 5: 1119–27.
- Urs NM, Bido S, Peterson SM, Daigle TL, Bass CE, Gainetdinov RR, et al. Targeting beta-arrestin2 in the treatment of L-DOPA-induced dyskinesia in Parkinson's disease. *Proc Natl Acad Sci U S A* 2015; 112: E2517–26.
- Vaikath NN, Majbour NK, Paleologou KE, Ardah MT, van Dam E, van de Berg WD, et al. Generation and characterization of novel conformation-specific monoclonal antibodies for alpha-synuclein pathology. *Neurobiol Dis* 2015; 79: 81–99.
- Van Den Berge N, Ferreira N, Gram H, Mikkelsen TW, Alstrup AKO, Casadei N, et al. Evidence for bidirectional and trans-synaptic parasympathetic and sympathetic propagation of alpha-synuclein in rats. *Acta Neuropathol* 2019; 138: 535–50.